Failure Mechanism and Damage Characterization in Axially Crushed AlMg3.5Mn Aluminium Tubes

Shakeri, H. R.; Rahem, A.; Worswick, M. J.; Mayer, R.

The 45th International Conference of Metallurgists (COM 2006) [Proceedings], 2006-10-05

FAILURE MECHANISM AND DAMAGE CHARACTERIZATION IN AXIALLY CRUSHED AlMg3.5Mn ALUMINIUM TUBES

H. R. Shakeri and A. Rahem
Aluminium Technology Centre, NRC
501 Université Boulevard East
Chicoutimi, Quebec, Canada G7H 8C3
hamid.shakeri@cnrc-nrc.gc.ca

M.J. Worswick
Department of Mechanical Engineering
University of Waterloo
Waterloo, Ontario, Canada N2L 3G1

R. Mayer
Vehicle Development Research Lab, GM R&D Center.
30500 Mount Road, P.O. Box 9055
Warren, MI, U.S.A. 48090-9055

ABSTRACT

The current focus of research and development in transportation industry is to use lightweight materials such as aluminium alloys for more structural components. In this regard, maintaining safety of the passenger and vehicle is the most important, therefore crashworthiness of components made of lightweight materials must be evaluated prior to sizable application of these materials. The focus of the present study is to understand failure and damage mechanisms during the axial crushing of aluminium tubes made of AlMg3.5Mn alloy of 2 and 3.5 mm thickness. Due mainly to complexity of the crushed tubes, a microstructural approach is considered. In this study optical, stereo as well as scanning electron microscopy techniques have been used to study damage and failure mechanisms in these types of tubes, which are essential energy absorbing components in passenger vehicles.

INTRODUCTION

In recent years transportation industry has been in ever-challenging situation as contradicting needs have been imposed to the industry. To comply with the existing environmental regulations and economical constraints weight reduction has become a major axis of research and development. At the same time, the industry must also conform to existing crashworthiness regulations [1].

Consequently two issues should be addressed prior to considerable application of aluminium alloys in structural components. The first issue is the low formability of aluminium alloys compared to steel. The second issue related to assessing crashworthiness of aluminium alloys. In terms of formability, in general, hydroforming has been considered as a very promising method and therefore it is logical to consider tube hydroforming as a manufacturing process for fabricating components with the complex 3D shapes made of aluminium alloys, including tubes to be used for energy absorbing components or other structural applications. According to previous studies, low cost, lightness, ease of construction and a high-energy absorption density with a constant average collapse load at failure are important characteristics for an energy absorbing components [2]. The first three characteristics are clearly feasible for metallic tubes. However the energy absorption capacity will also depend on the amount of plastic deformation that occurs under axial loading. Therefore in addition to geometrical parameters such as internal/external diameters, thickness and length of the tube, strain-hardening characteristics of the tube material both during the manufacturing as well as axial crushing is also very important.

In general, automotive structural behaviour during a crash event is a complex problem due mainly to the highly non-linear behaviour of structures in crash. Reliable methods to quantitatively assess the problem are being developed, but experimental approaches, such as prototype components, specimens, etc., to understand crash behaviour, are still necessary in vehicle design [3]. Axial collapse of cylindrical tubes, as a simple energy absorbing component, under quasi-static loading is extensively studied both experimentally and numerically and is classified in seven collapse modes as shown in Figure 1 [2]. As the figure suggests, the length to diameter and thickness to diameter ratios determine the resulting collapse mode. Further investigation has shown that axially crushed tubes are most efficient impact energy-absorbing component when deforming into concertina or multi-lobe mode of collapse [4].

In recent years there has been more emphasis on the crashworthiness of the hydroformed aluminium tubes using finite element simulations alongside experimental works. For instance in case of low and high pressure hydroforming processes on aluminium alloy tubes, it was found that the energy absorption during the impact decreases with decreasing corner-fill of the hydroformed tube [5].

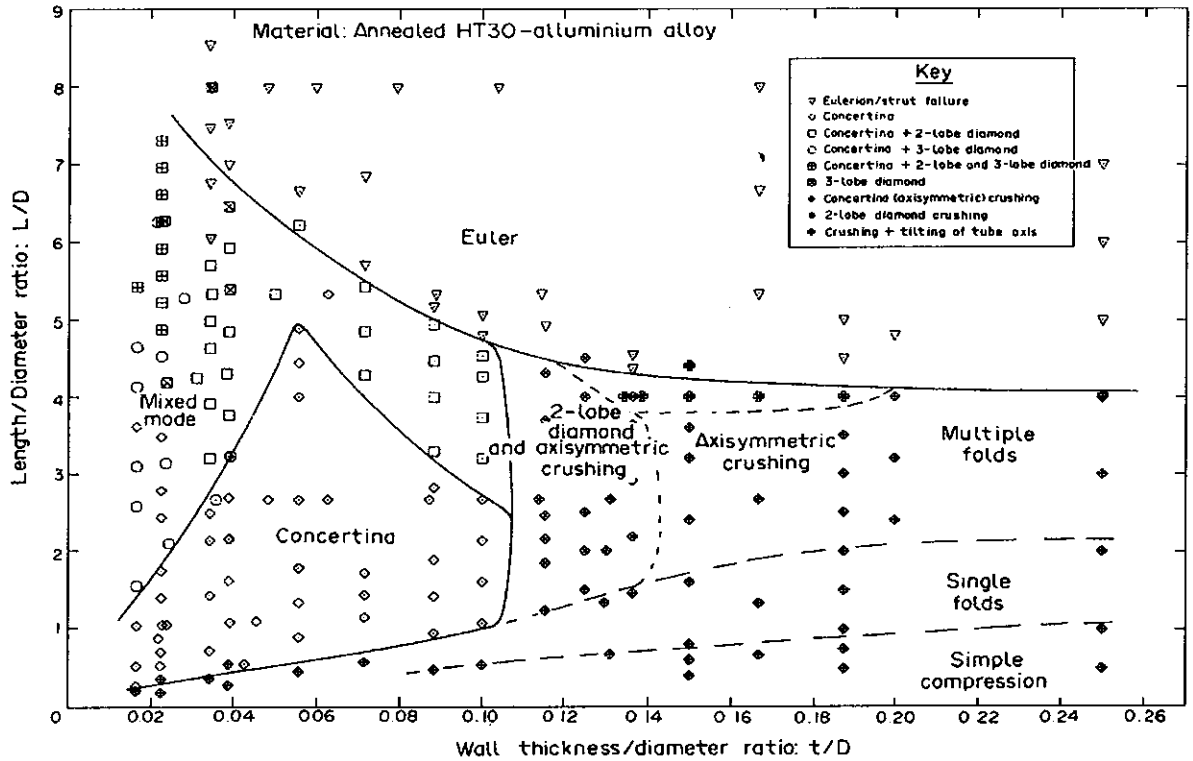

Figure 1 – Classification chart of the collapse modes in axially crushed aluminium (HT-30) tubes [2]

In dealing with crashworthiness simulations a comprehensive approach for predicting failure in a component based on macroscopic strains and stresses is also examined. The latter approach requires the use of a number of different failure mechanism representations, such as necking, as well as ductile and shear. However, using such a failure approach one can only predict the crack initiation [6]. Therefore, it is necessary to understand the actual complex deformation and failure mechanisms in a crushing tube in order to have better failure criteria input for finite element simulations. The present investigation takes a microstructural approach to study damage initiation and failure mechanisms in axially crushed cylindrical aluminium tubes prior to perform such study on hydroformed aluminium tubes.

EXPERIMENTAL PROCEDURE

For the present investigation tubes made of AlMg3.5Mn aluminium alloy were examined. The original dimensions of the tubes were 76.2 mm diameter, 400 mm length and 2 or 3.5 mm wall thickness. Figure 2 shows the typical stress-strain curve for this type of alloy. The tubes were axially crushed at GM's R&D Centre using a drop tower. In order to facilitate axial crushing, prior to the test, aluminium plates were welded at two ends of the tubes as shown in Figure 3a. Two sets of 2 and 3.5 mm thick axially

crushed tubes are shown in Figures 3b and c, respectively. Figure 4 shows typical crush force-distance curves obtained for 2 and 3.5 mm thick axially crushed tubes.

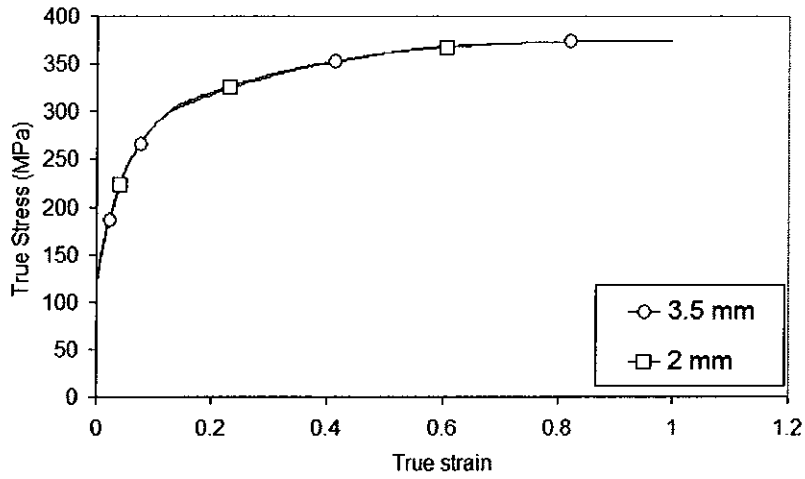

Figure 2 – A typical stress-strain curve for the aluminium alloy under consideration

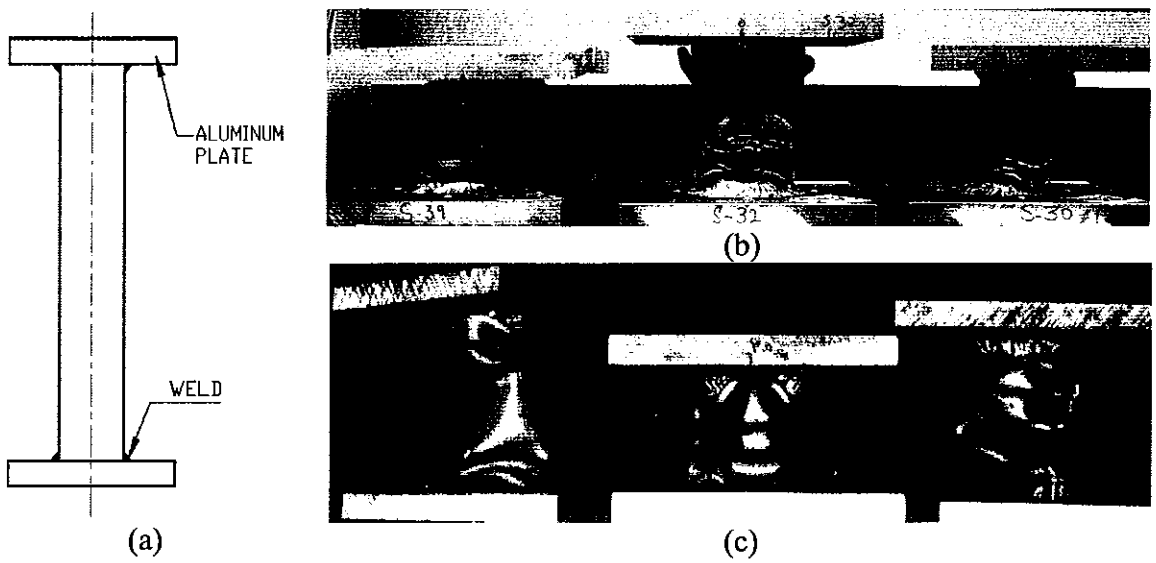

Figure 3 (a) schematic of the original tubes with aluminium plates welded at the two ends, (b) and (c) sets of axially crushed 2 and 3.5 mm thick tubes, respectively.

Due mainly to complexity of the tubes, the test specimens were sectioned at multiple locations as shown in Figure 5. Actual sectioning was done using abrasive cut-of-wheel. Afterwards the sections cold mounted, mechanically grinded and polished before optical microscopy. Figure 6 shows several cross sections of the mounted specimens, as indicated in each image all folded as well as fractured segments were given a number and examined under the microscope. Occasionally sections include partially or fully fractured segments that provide clues on fracture micromechanism.

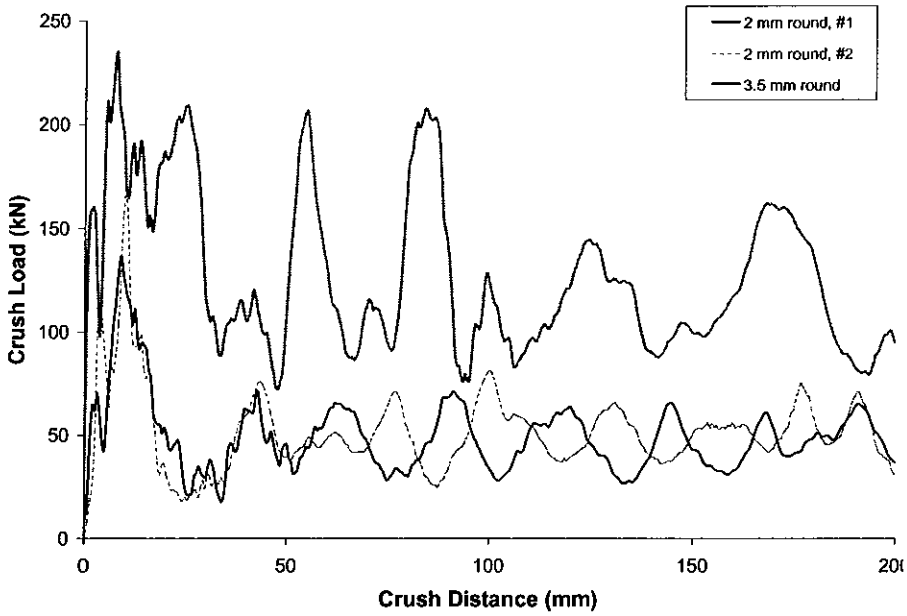

Figure 4 – Several typical load-distance curves for 2 and 3.5 mm axially crushed tubes

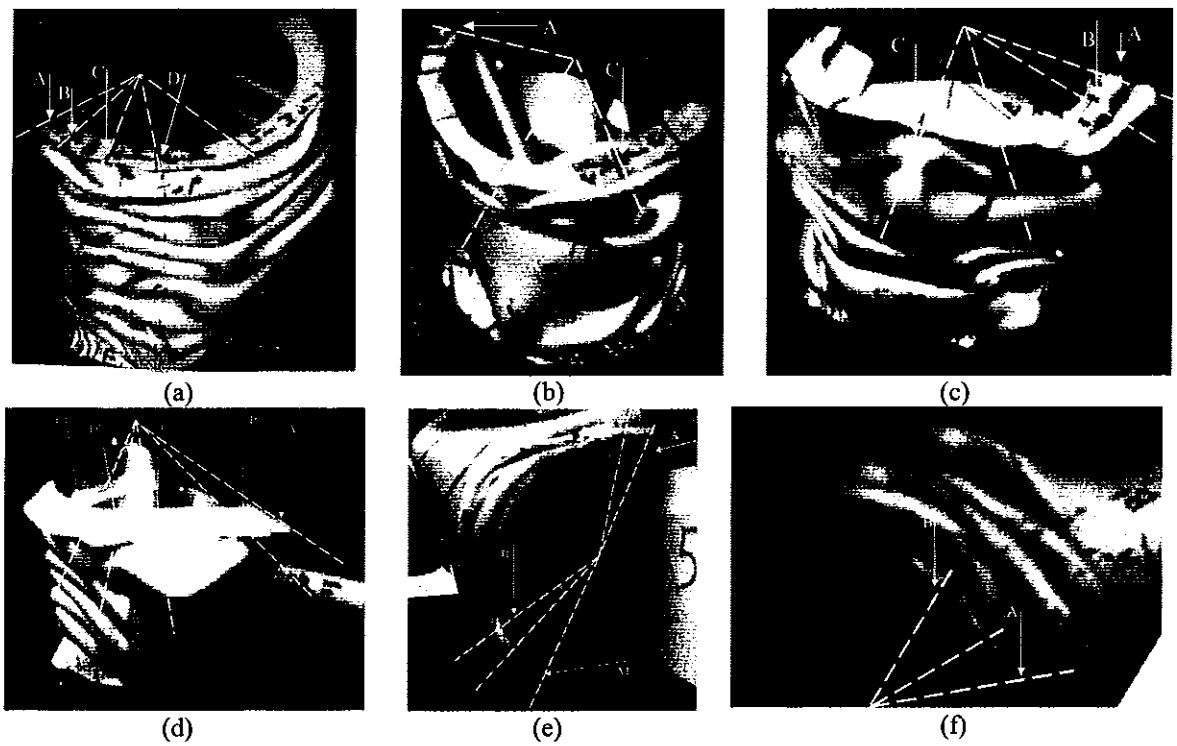

Figure 5 – Sectioning of the specimens for optical microscopy is done along the radial lines shown in (a)- (c) 2 mm thick specimens S-30, S-32 and S-39

respectively; and (d)-(f) 3.5 mm thick tubes S-43, S-45, and S-28, respectively

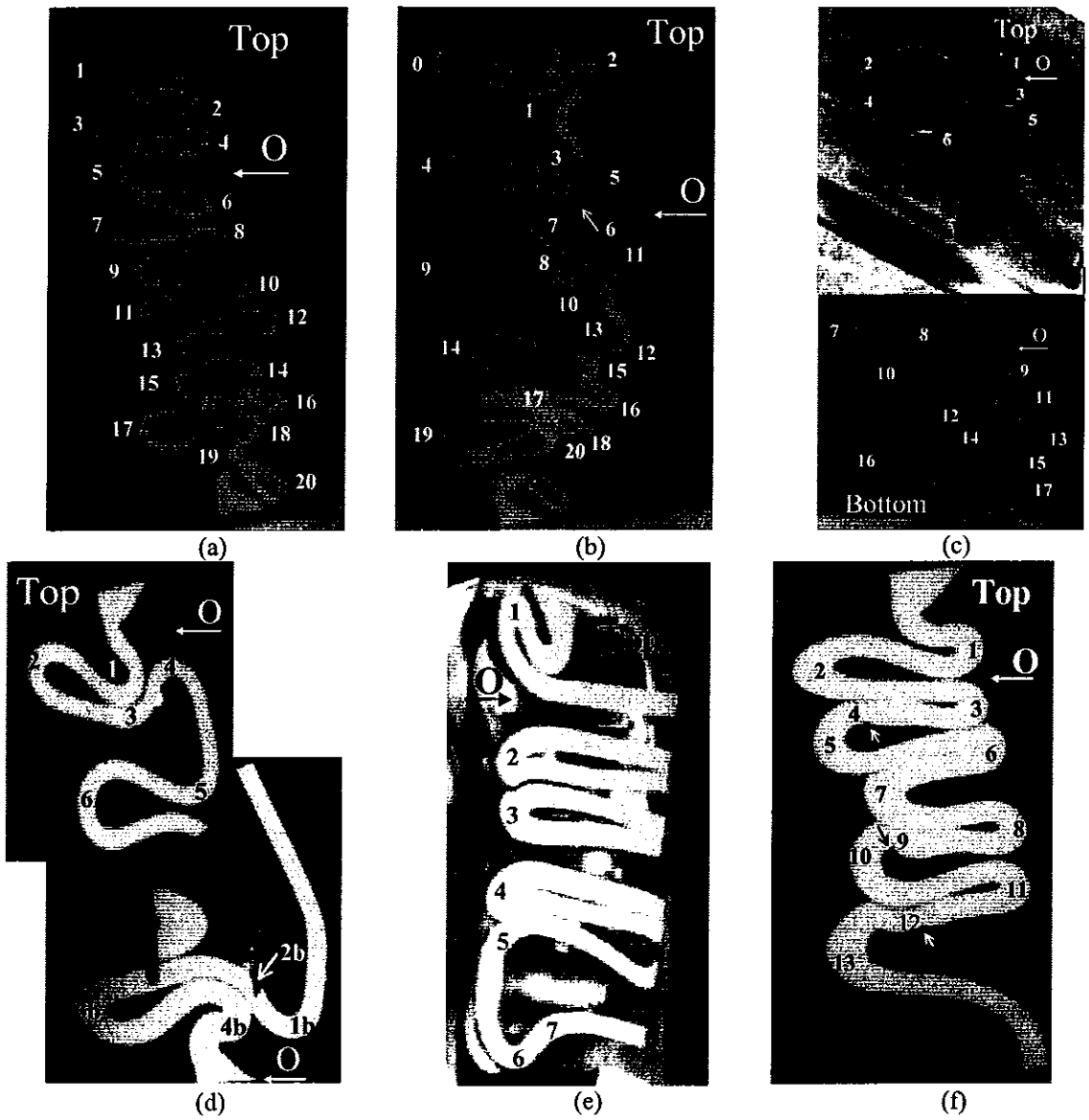

Figure 6 – Some of the mounted sections the specimens are shown here, (a), (b) and (c) are from 2 mm thick tubes and (d), (e) and (f) are from 3.5 mm tubes. The letter "O" indicates the outside of the tubes and also the topside is also marked; (a) specimen S-30 section C, (b) specimen S-30 section D, (c) specimen S-32 section A, (d) specimen S-28 section A, (e) specimen S-43 section D, and (f) specimen S-45 section B.

It seems that whenever several folded segments align under each other they might act like a cutting tool shearing the next neighbouring folding segment. In addition during the folding sequence the contact between different folding segments might produce a

"locking effect" for a neighbouring segment limiting the flow of the material in that segment leading to fracture. Adding to the complexity of the situation, it is also possible that two ends of the tube do not remain parallel, during the crash test, and add shearing, tearing component or a combination of the two into the equation.

RESULTS AND DISCUSSION

Optical Microscope Examination

Since each specimen contains multiple folds to obtain a realistic understanding of the material flow, damage and final failure it is necessary to examine a large number of folded segments. In general the bending radius for each fold is important, in addition the interaction of each folding segment with the neighbouring segments also plays an important role as it may impose additional constraint or alter friction parameters. Therefore, it has been tried to separate simple folding cases from those influenced by the interaction from the adjacent segments.

During the examination of the 2mm as well as 3.5 mm round tubes, similar common features were observed. Figure 7, illustrates some of these common features. One of these common features is concentration of the damage at the inner side of the folded segments in form of squeezed out with fishtail morphology. In addition, branched and blunt cracks that were detected in all specimens. Also the outer part of the folded segments (deformed in tension) hardly shows any significant sign of damage unless there are additional constraints imposed by an impact from one or more neighbouring segments, while the inner segments that are in compression consistently exhibit tremendous amount of materials flow toward the centre of the bend and as a result at the inner edges numerous cracks are observable that produces fish-tail or tooth-like sub-segments. Loss of inner bend symmetry as a result of interaction with neighbouring segment is another common feature in these specimens. It should be noted that in cases such as the one shown in Figure 7 c, d and e, the direction of crack growth and materials flow are against each other. In another word, as the cracks moves toward the centre of the thickness it enters the material that is both less compressed and less strain-hardened.

In case of interaction with the neighbouring segments unlike the simple bending condition evidences of damage often are observable in inner as well as outer part of a folded segment. Asymmetry of the bend as a result of the impact as well as formation of the larger cracks, which are slanted to the opposite direction of the impact, was also observed. Another frequently observed features in these sections have been blunt cracks as shown in Figure 7. The reason for the occurrence of these cracks is not clear yet. There are a few possible explanations for the blunt cracks. One possibility might be the spring back of the tube after the test.

Failure Mechanisms

A. Metallographic Observations

Mechanism of damage and failure in these crushed aluminium tubes is the main topic of this section. One of the difficulties associated with identifying failure mechanism

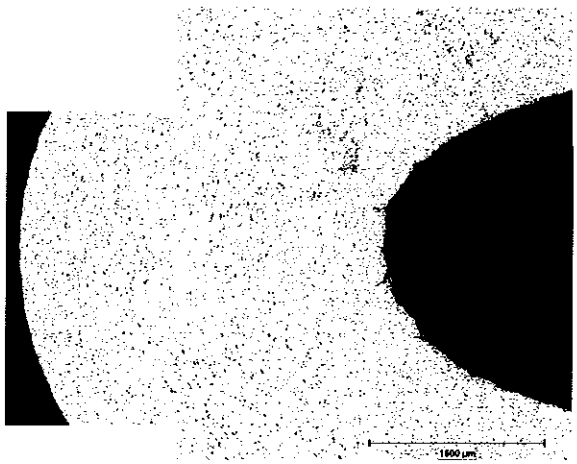

(a)

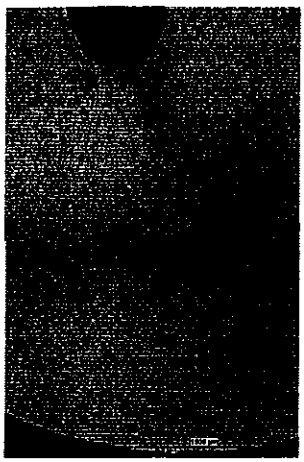

(b)

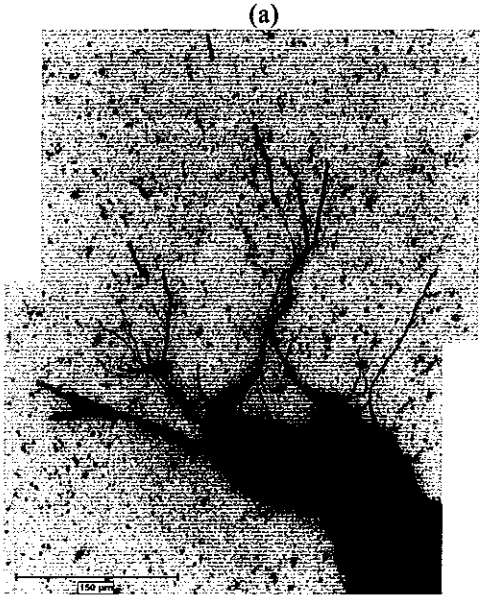

(c)

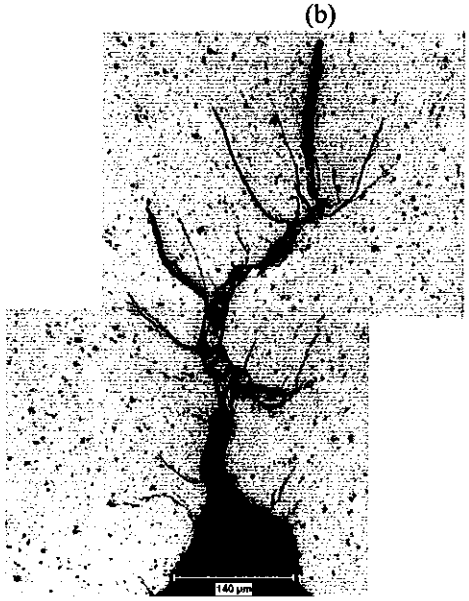

(d)

(e)

Figure 7 – Some of the segments with typical features that were frequently observed, (a) 2 mm thick specimen S-39 section "Ct" #4, (b) 3.5 mm thick specimen S-45 Section "B" #1., (c) 2 mm thick specimen S-32 section "A" #15, (d) 3.5 mm thick specimen S-43 section "D" #3, and (e) 3.5 mm specimen S-43 section "A" #3.

is unknown sequence of events. Metallographic examination of the sections cut from the tube is helpful specially in determining the micro-mechanism of damage, however such information must be viewed along with the loading condition in a tube in general and in each fractured segment in particular and in the present case the situation is complex rather than simple. The situation became further complicated due to lateral movement of the tube during the test. From this point some of the fracture and failure cases observed in these tubes will be summarized.

Figure 8 shows a series of mostly composite images of the fractured segments in 2 mm thick axially crushed tubes. Some of the segments shown in the figure clearly exhibit characteristics of a segment failed under shear. For instance, the cases shown in Figures 8a, c, and d are clearly clear cases of shear type of failure. In Figures 8b, e, f and g some of the characteristics of a case of fracture under shear are present but the clear necking in 8b, mismatch of the two parts of the failed segment in 8e, f and g could be result of other loading modes or at least a mixed mode of failure. Segment shown in Figure 8h does not exhibit characteristics of a segment fractured under shear. In most of the cases shown in Figure 8 it is clear that an impact from a neighbouring segment contribute to the fracture. In Figure 8c the direction of the impact is shown by an arrow and the shearing forces are also shown by the arrows near the failed segment, which has failed as a result of constraint imposed by the nearby folded segment as well as the impact from the adjacent segment. The insert included in Figure 8e is the higher magnification of the area pointed by the arrow that shows the tip of the fracture region. This suggests a rough rather than smooth surface as a result of zigzag fracture direction.

Similarly, Figure 9 is a series of composite images of some of the fractured segments in 3.5 mm thick tubes. In general, the fractured segments are very similar to those in 2 mm thick tubes. Once again the role of impact from the adjacent segments is evident. In most cases, fractured segments show the characteristics of a shear type of failure. In cases like the one shown in Figure 9b, due to the mismatch between the two side of the failed segments, fracture through a purely shear mechanism is unlikely. This observation is also supported by the zigzag morphology at the tip of the fractured regions in Figures 9b and d, similar to the one in Figure 8e, which are shown in a higher

magnification in Figure 10. This might suggest that after partial fracture through shear mechanism, local loading condition at the tip of the fractured region changes due perhaps to consequential folding of the tube during the axial crushing.

In this section it is also important to focus on microscopic aspect of damage and failure of these tubes. Figure 11is one example of particle induced damage in 2mm thick specimen S-30 section that provides evidence for shear type of flow and failure in this case. Details of the failed region as shown in Figure 11 b and c clearly illustrate the role of particles in form of particle-induced damage leading to final failure. Evidences of similar type of failure in 3.5 mm tubes were also observed.

B. Stereomicroscope Observations

Examination of some of the sections using stereomicroscope provides supporting evidences that are complimentary to the observations reported in the previous section on optical microscopy.

(a)

(c)

(b)

(d)

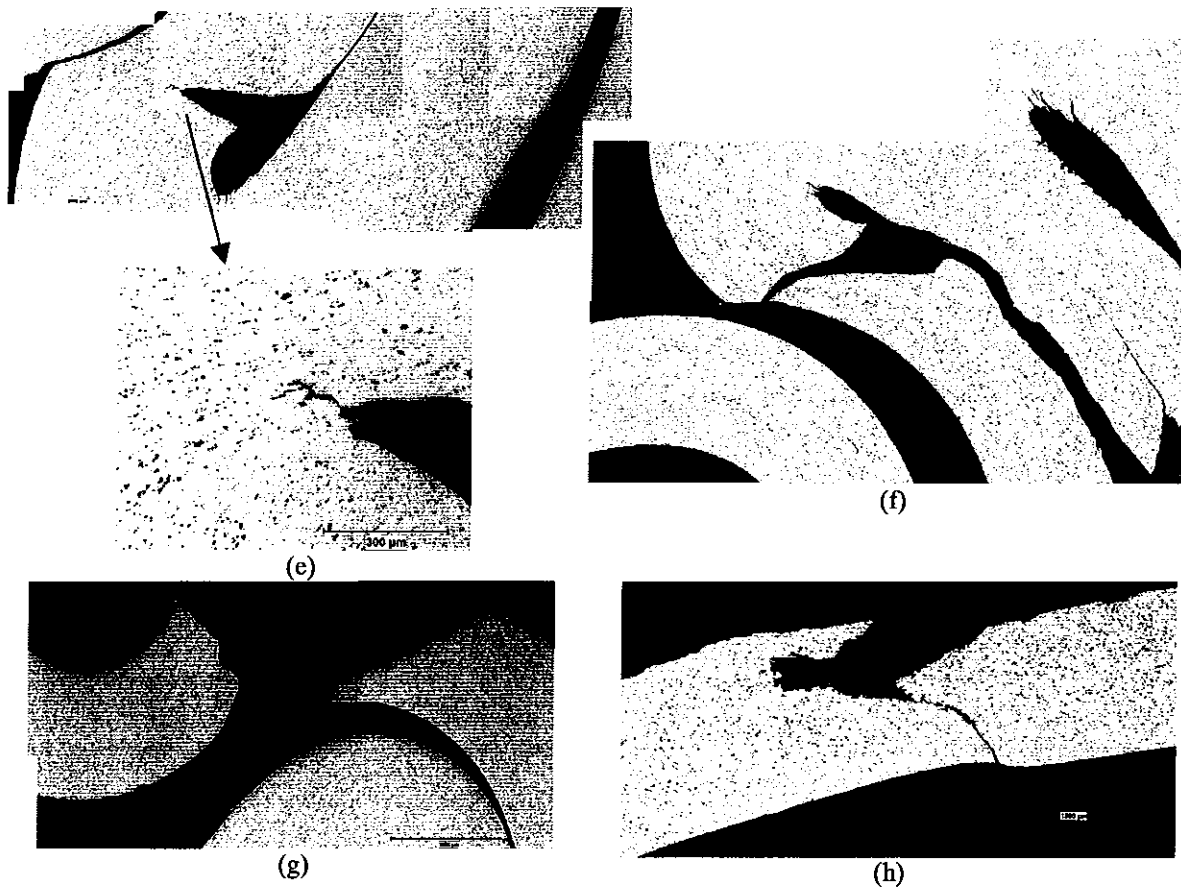

Figure 8 – Fractured segments in 2mm thick specimens, (a) S-30 section A # 4, (b) S-39 section B #10, (c) S-30 section A #16, (d) S-32 section Ct #5, (e) S-30 section D #18, (f) S-39 section A #4, 4a, 5and 6, (g) S-39 section B #3, and (h) S-39 section Ct #5.

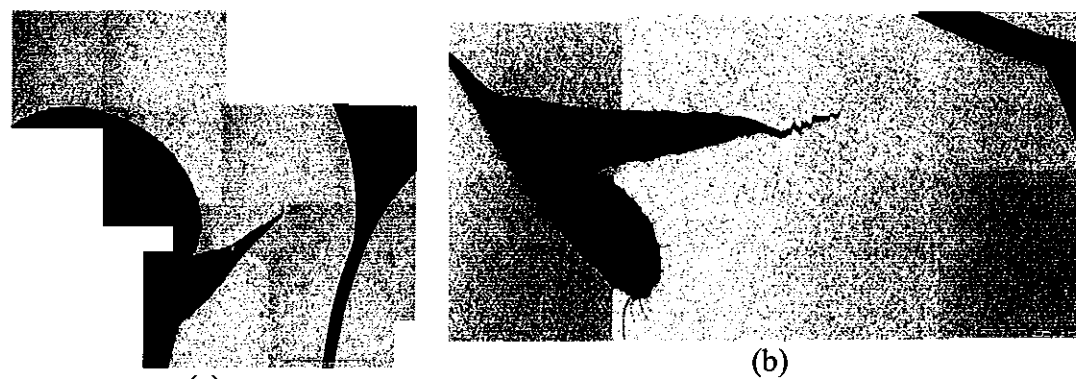

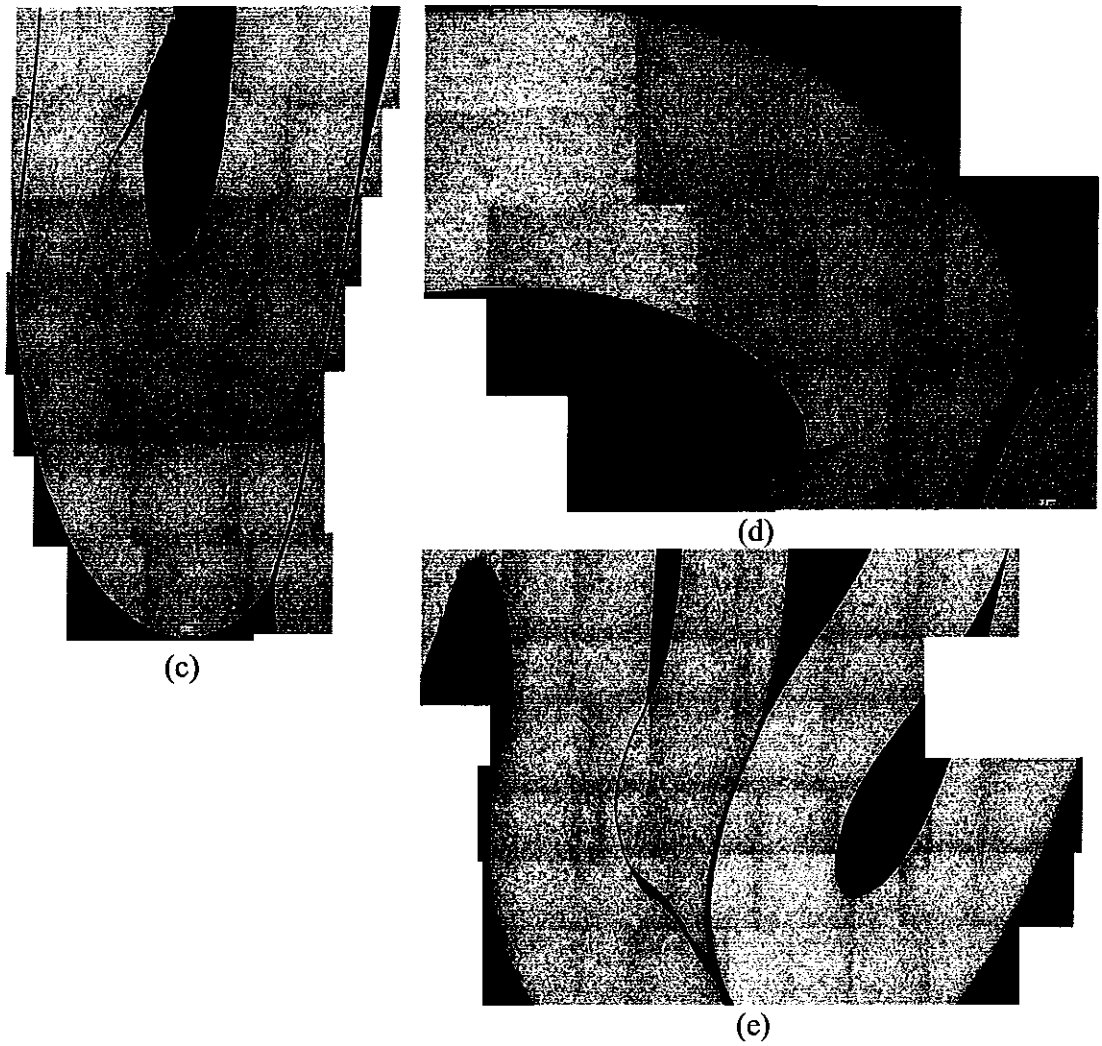

Figure 9 – Fractured segments in 3.5 mm thick tubes, (a) S-28 section B #7, (b) S-28 section B #3, (c) S-43 section E #8 & 9, (d) S-45 section A1 #3 & 2, and (e) S-45 section A #3, 5 & 6

As could be seen from several sections of the specimens shown in Figure 12 the interaction between neighbouring segments plays an important role in failure process.

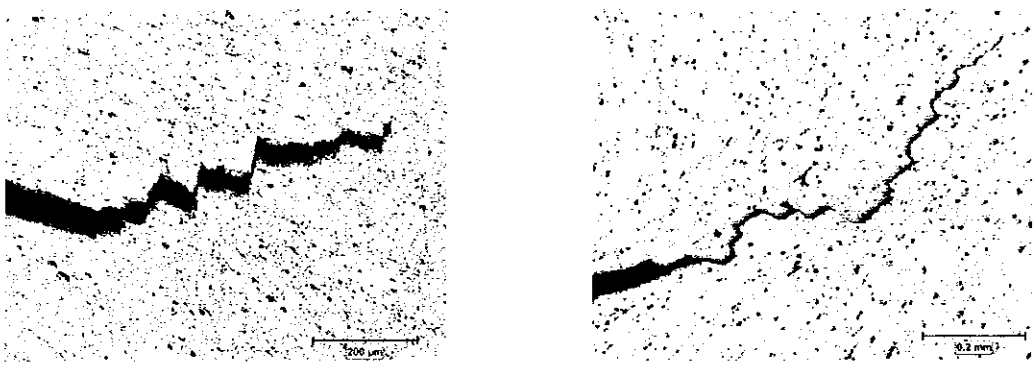

(a) (b)

Figure 10 – Tip of the fractured region in segments shown in (a) Figure 9b and (b) Figure 9d.

The segment in Figure 12a apparently failed as result of a combination of tension and tearing (opening and tearing mode of loading). The segment shown in Figure 12b shows the characteristics of shear type of failure (sliding mode of loading). Finally the obvious mismatch between the two sides of the failed segment shown in Figure 12c indicates that a mixed mode of loading caused the failure. While one side clearly illustrates the characteristics of a segment failed under shear, the other side does not show similar characteristics. Figure 12 d suggests that the upper fold on the image failed under shear while impacted by the lower fold. The appearance of the failed segment implies that the upper part might have slightly stretched over the lower fold prior to failure and upon fracture the residual stresses caused by earlier folding of the upper part is released that is why the failed edge slightly curved counter clockwise. Segment shown in Figure 12e is evidence of failure under mode II, sliding mode, of failure and again the additional constraint due to earlier folding play an important role in local loading as well as final failure. Figure 12 f shows a segment failed as result of impact from the neighbouring folded segment that generated a combination of stretching and tension in the failed segment. The latter case exhibits the characteristics of a shear type of failure.

C. Scanning Electron Microscopy

Several failed segments were removed from the crushed tubes and examined using SEM. One example is a failed segment from the bottom second fold of 2mm thick specimen S-39, shown in Figure 13a and b. In this case shallow oriented dimples typical of fracture surfaces produced under shear or tear are observable as shown in Figure 13b. Figure 13c and d show a failed segments in 3.5mm thick specimen S-28 at low and high magnification, respectively. Low as well as higher magnification view of the dimple morphology in this specimen suggests that the main failure mechanism at this location is mainly shear type. In another case in 2mm thick specimen S-39 a folded segment failed as a result of a second bending in a direction normal to the primary folding direction as shown in Figure 13e. Elongated dimples are observable in this segment as shown in Figure 13f. The segment also illustrates a set of secondary cracks normal to the primary fracture surface that supports mixed mode of loading.

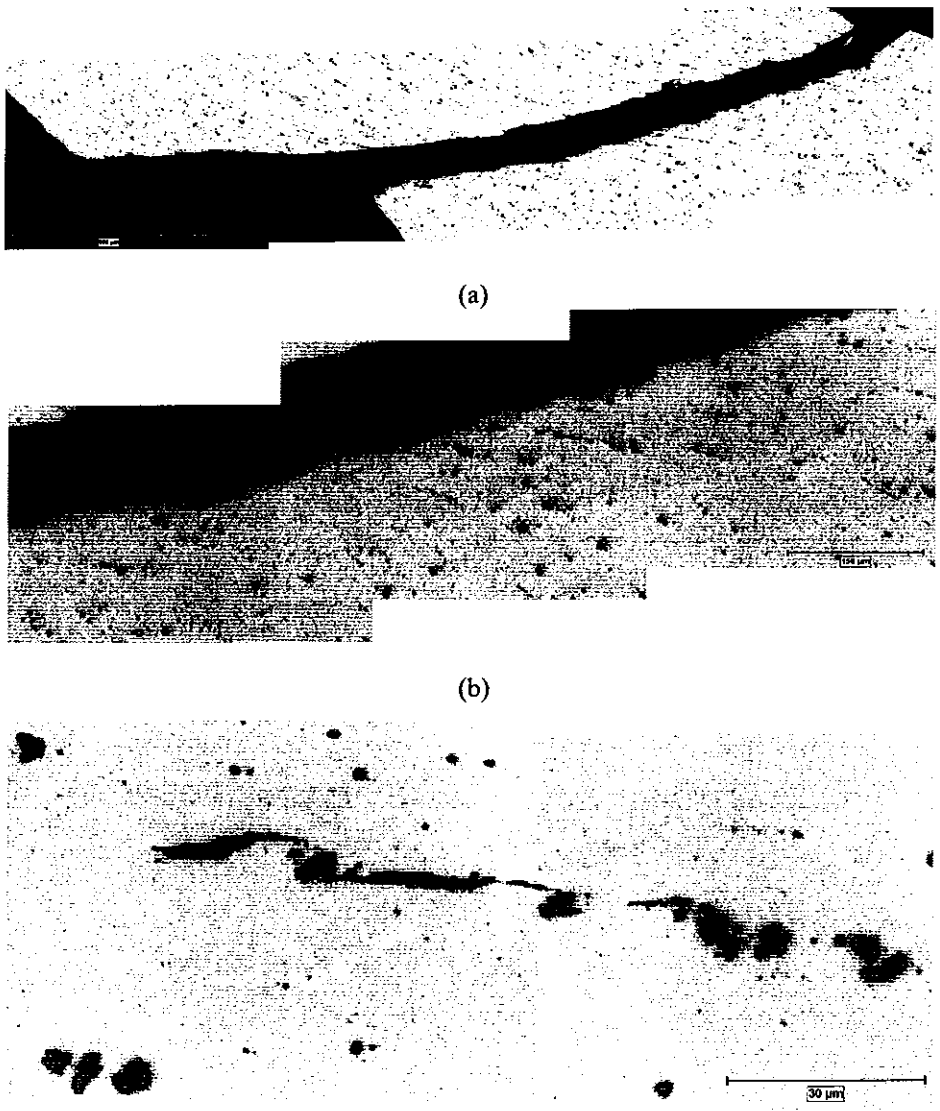

(a)

(b)

(c)

Figure 11 – Fracture edges in 2 mm thick tube S-30 section A #13, (a) general view, (b) flow of the material and convergence of the flow line as well as particle stringers, and (c) particle induced damage in one of the stringers.

In general in terms of failure mechanisms in axially crushed tubes, the results for 3.5 tubes are very similar to the one for 2 mm tubes of the same alloy. It seems that, the 3.5 mm tubes failed more consistently, although occasionally they have shown unusual failure cases. However, it should be noted that the length of the original tubes prior to the axial crushing for both thickness maintained the same that might have affected the collapsing mode in the 3.5 mm tubes.

CONCLUSIONS

After all examination of the tubes it is clear that the deformation and failure are very complex due to complex phenomena occurred during axial crushing. Therefore, it is difficult to point at a single failure mechanism as the cause of failure. A segment might initially fail by one mechanism and failure might propagate by another mechanism. Nevertheless, it is fair to say that shear type of failure could be pointed out as the most frequently observed failure mechanism. This assessment is compatible not only with the general nature of the axial crushing but also with the microscopic observation reviewed herein. Specifically, it has been possible to view the very early stage of the shear failure in partially sheared segments frequently observed in the vicinity of the main failure surfaces. Figure 14 shows one of these partially sheared segments.

In addition based on the result of the present study the following conclusions could be made for 2 and 3.5 mm round tubes:

- Failure mechanism follows the complexity of the local loading condition.
- In 2 mm thick tubes although shear is the only failure mechanism that could be isolated and pointed out, considering the morphology of the failed segments in general and occasional mismatch in particular along with microscopic observations, other failure mechanisms could not be ruled out. At least in some cases a mixed mode of failure is active. In majority of the cases in 3.5 mm thick tubes, shear was recognized as the main failure mechanism.
- Failure is more consistent in 3.5 mm tubes compared to 2mm tubes, however that might be as a result of maintaining the same original length for both thicknesses.
- Strong influence of the impact from the neighbouring segment has been observed in all tubes.
- Regardless of the acting failure mechanisms, significant amount of particle-induced damage has been observed in fractured segments.
- Also the observations reported herein support the previous findings [7] of that most of the damage concentrated on the inner side of the folded segments.

ACKNOWLEDGMENTS

The authors would like to express their gratitude to General Motors and National Research Council Canada for granting permission for publication of the result of the present investigation.

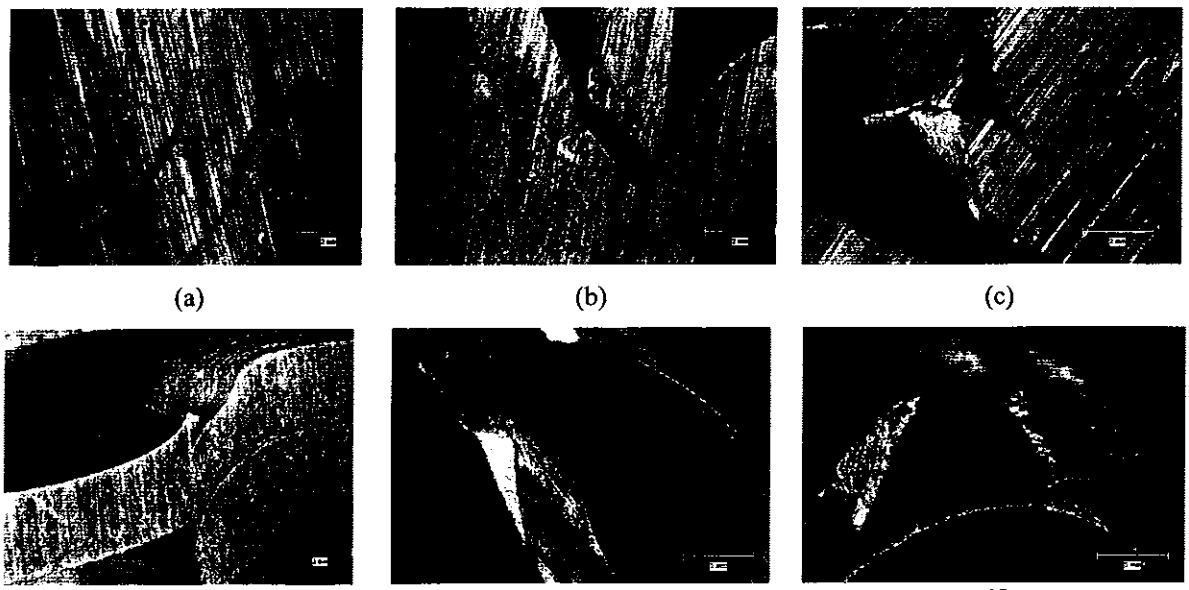

Figure 12 – (a) to (f) several stereomicroscopic images of the failed segments in the axially crushed tubes

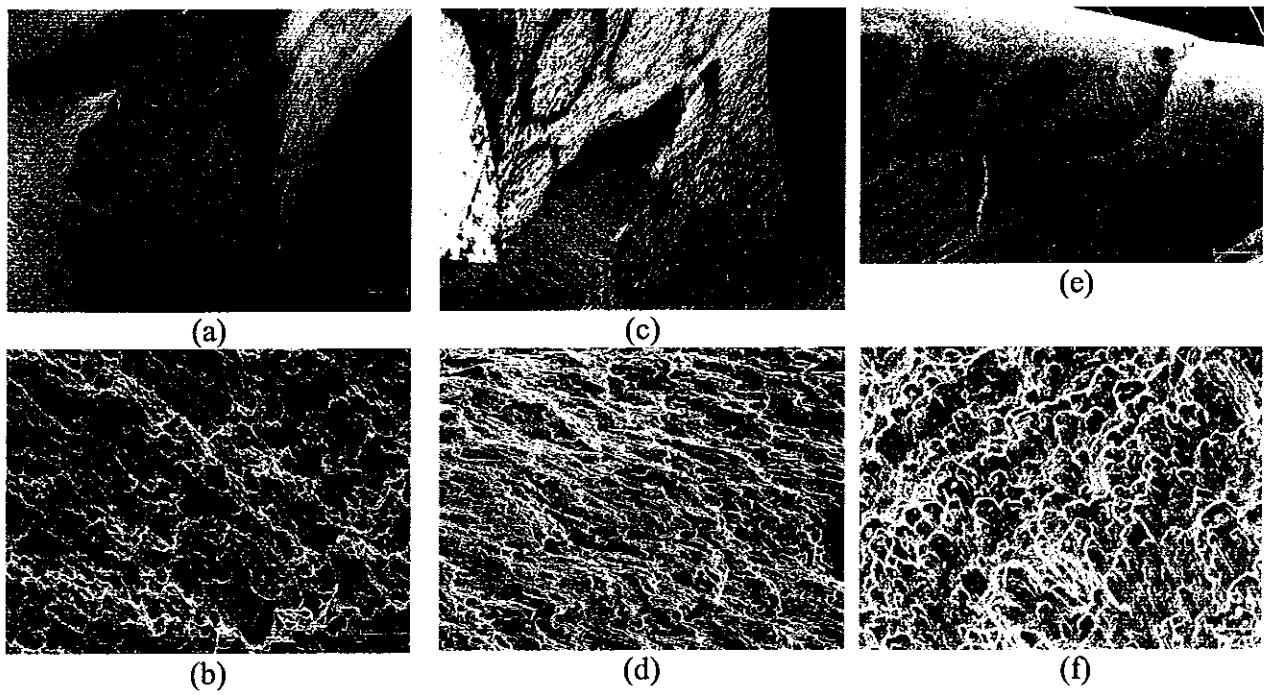

Figure 13 Fracture surfaces in failed segments, (a) and (b) 2mm thick specimen S-39, (c) and (d) 3.5 mm specimen S-28, (e) and (f) another failed segment in specimen S-39.

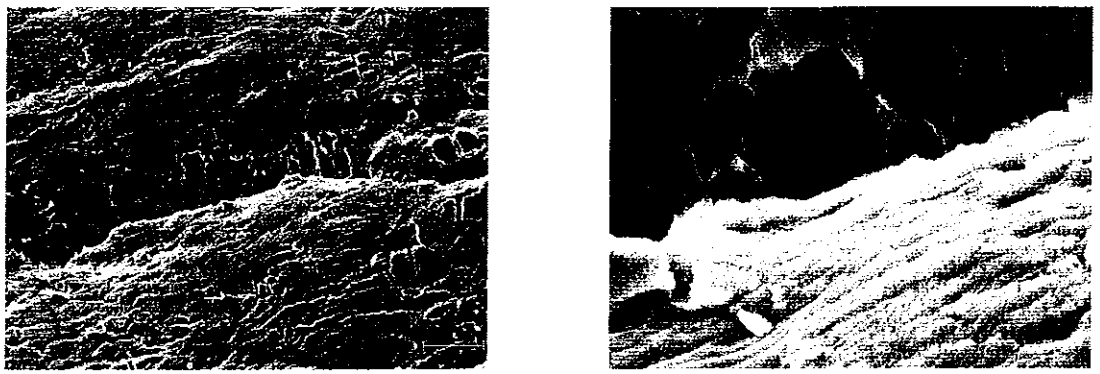

(a) (b)

Figure 14 – (a) a partially failed area in specimen S-39, (b) higher magnification of the fracture surface showing the elongated dimples

REFERENCES

1. A.G. Hanssen, L. Lorenzi, K. K. Berger, O. S. Hopperstad, and M. Langseth, " A Demonstrator Bumper System Based on Aluminium Foam Filled Crash Boxes", I. J. Crash, Vol. 5 (2000), No. 4, pp. 381-392.
2. K. R. F. Andrews, G. L. England, and E. Ghani, "Classification of the Axial Collapse of Cylindrical Tubes under Quasi-Static Loading", Int. J. Mech. Sci., Vol. 25 (1983), No. 9-10, pp. 687-696.
3. N. Jones and T. Wierzbicki, Structural Crashworthiness, Butterworth & Co Ltd., London, England, 1983, p.96.
4. Singace, and H. El-Sobky, "Interplay of Factors Influencing Collapse Modes in Axially Crushed Tubes", I. J. Crash, Vol. 5 (2000), No. 3, pp. 279-97.
5. W. Williams, D. A. Oliveira, M. J. Worswick, and R. Mayer, "Crashworthiness of High and Low Pressure Hydroformed Straight Section Aluminium Tubes", SAE Technical Paper # 2005-01-0095.
6. H. Hooputra, H. Gese, H. Dell, and H Werner, "A Comprehensive Failure Model For Crashworthiness Simulation of Aluminium Extrusions", I. J. Crash, Vol. 9 (2004), No. 5, pp. 449-463.
7. H. R. Shakeri, M.J. Worswick, and R. Mayer, "Failure Mechanism and Damage Characterization in Crash-Tested Aluminium Tubes", in "Proceedings of Canadian Aeronautics and Space Institute18th Aerospace Structures and Materials Symposium", Toronto, Ontario, 26-27 April 2005.